Host–Guest Systems

DOI: 10.1002/ange.201210373

Switchable Nanoporous Sheets by the Aqueous Self-Assembly of Aromatic Macrobicycles**

*Yongju Kim, Suyong Shin, Taehoon Kim, Dongseon Lee, Chaok Seok, and Myongsoo Lee**

The molecular self-assembly of aromatic building blocks is a powerful approach to the construction of dynamic nanostructures that are able to respond to external stimuli by changing their shape and/or macroscopic properties.[1] In this context, it is possible to modulate the interplay between multiple noncovalent interactions through the rational design of molecular modules. The directionality of these interactions plays a critical role in controlling the shape of the self-assembled structures.[2] Laterally grafted rod building blocks lead to one-dimensional nanofibers through unidirectional guiding of the elongated aromatic rods in the self-assembly process.[3] Anisotropic micelles also undergo directional growth to form low-dimensional supramolecular structures in selected solvents.[4] For example, hydrophobic oblate micelles with hydrophilic side faces stack on top of each other to form 1D nanofibers.[5] On the other hand, hydrophobic aromatic rod bundles with hydrophilic up and down grow through side-to-side interactions to form freely suspended 2D structures in bulk solution.[6] A reduction in the strength of the aromatic interactions leads the resulting planar sheets to form 2D networks.

However, the elaborate construction of 2D structures requires the rational design of molecular building blocks that are able to grow in two dimensions. One possibility is the side-by-side arrangement of 2D molecular building blocks, such as flat disk-shaped aromatic molecules. Nonetheless, most flat aromatic amphiphiles stack together through face-to-face interactions to form nanofibers.[2a,7] To frustrate continuous aromatic stacking in one dimension, one can introduce flexible chains on the basal plane of the aromatic structures. The basal-plane chains should enforce a lateral arrangement of the flat aromatic segments and their two-dimensional growth rather than growth through conventional 1D aromatic stacking (Figure 1). With this idea in mind, we designed a flat aromatic bicycle with a hydrophilic dendron at the center of the basal plane. Another important issue regarding 2D planar structures is the possibility of the integration of dynamic response characteristics triggered by environmental changes. The combination of principles of 2D planar structures with responsive properties would generate a new class of intelligent nanomaterials.

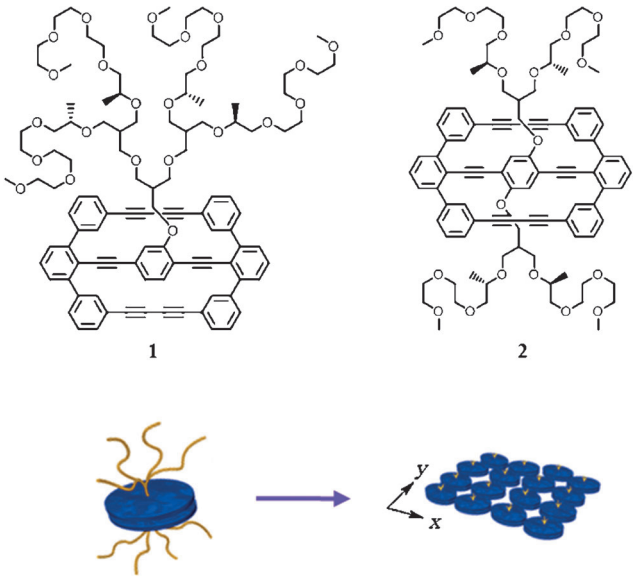

Figure 1. Molecular structure of aromatic macrobicycles with dendrons attached to their basal plane and schematic representation of the 2D growth of the flat micelles derived by pairwise stacking.

Herein we report the spontaneous formation of 2D porous sheets in aqueous solution through the two-dimensional self-assembly of an aromatic macrobicycle with a hydrophilic dendron attached to its basal plane. Remarkably, unlike conventional nanoporous materials, the resulting porous sheets underwent dynamic motion between open and closed states, as triggered by guest intercalation (Figure 4).[8]

The self-assembling molecules that form this aggregate consist of a macrobicyclic aromatic segment and a hydrophilic oligoether dendron grafted at the center of the basal plane (Figure 1). The synthesis of the flat aromatic amphiphiles began with the Sonogashira coupling of a dendron-substituted diiodobenzene derivative with 2,6-dibromoethynylbenzene to provide a tetrabromo building block (see the Supporting Information). Suzuki coupling of the tetrabromo compound with 3-((triisopropylsilyl)ethynyl)phenylboronic acid ester, followed by silyl-group deprotection with tetra-*n*-butylammonium fluoride, then provided a precursor with four terminal alkyne groups. The final aromatic amphiphiles were synthesized efficiently by intramolecular Glaser-type coupling of the terminal alkyne groups under dilute reaction

[*] Y. Kim, T. Kim, Prof. M. Lee
State Key Laboratory of Supramolecular Structure and Materials
College of Chemistry, Jilin University
Changchun 130012 (P. R. China)
E-mail: mslee@jlu.edu.cn
S. Shin, D. Lee, Prof. C. Seok
Department of Chemistry, Seoul National University
Seoul 151-747 (Korea)

[**] This research was supported by the National Science Foundation of China (Grant No. 21221063), the Programme of Introducing Talents of Discipline to Universities (111 Project of China, B06009), and the Air Force Research Laboratory (FA2386-12-1-4078). We thank Prof. T.-L. Choi at SNU for his helpful input into this research.

Supporting information for this article is available on the WWW under http://dx.doi.org/10.1002/anie.201210373.

© 2013 Wiley-VCH Verlag GmbH & Co. KGaA, Weinheim

conditions ($CuCl/CuCl_2$ in pyridine).[9] The resulting molecules were characterized by ^1H and ^{13}C NMR spectroscopy and MALDI-TOF mass spectrometry and were shown to be in full agreement with the structures presented.

Molecule **1** self-assembles into nanoporous sheets in dilute aqueous solutions. Cryogenic transmission electron microscopy (cryo-TEM) showed sheetlike objects with curved edges against the vitrified solution background (Figure 2a); this observation is indicative of the formation of flexible sheets in bulk solution. Notably, a high-resolution

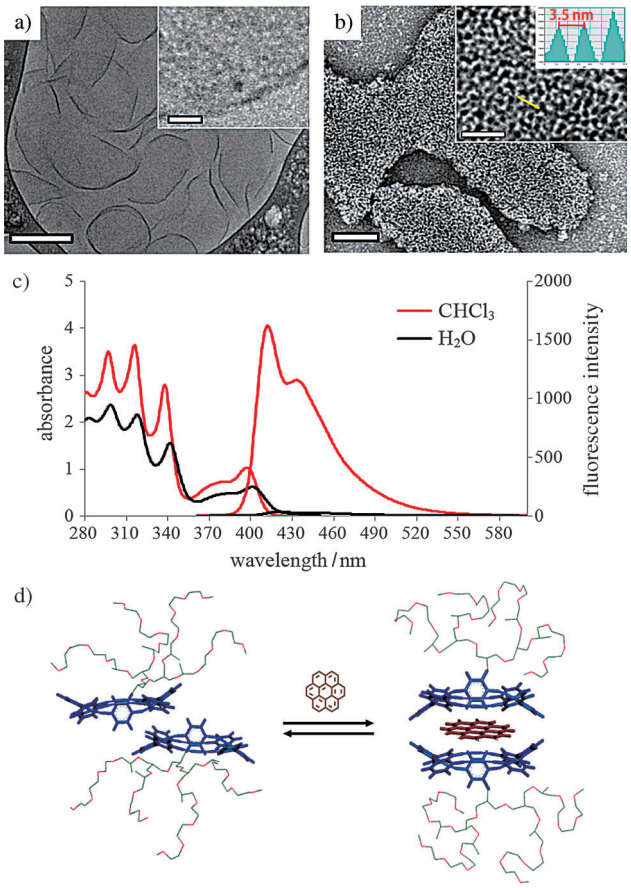

Figure 2. a) Cryo-TEM image of a solution of **1** (200 μM; scale bar: 200 nm). b) Negatively stained TEM image of nanoporous sheets from a 100 μM aqueous solution of **1** (scale bar: 100 nm). The insets in (a) and (b) show magnified images (scale bars: 20 nm) and the line scan profile along the yellow line. c) Absorption and emission spectra of **1** (100 μM) in $CHCl_3$ (red line) and aqueous solution (black line); $\lambda_{ex} = 318$ nm. d) Molecular modeling of the dimeric micelle without coronene and the dimeric micelle containing coronene.

image revealed that the sheets contained in-plane nanopores with an average diameter of approximately 4 nm (Figure 2a, inset). To obtain more information on these sheets, we also performed TEM experiments with the samples cast onto a TEM grid (and negatively stained with uranyl acetate). A low-magnification image showed planar sheets with rugged surfaces against a dark background. A higher-magnification image showed that the rugged surfaces consisted of uniform micelles and nanopores (Figure 2b, inset) and thus suggested that the sheets had formed through a lateral association of small, discrete micelles. The diameters of the micelles and the pores were measured to be approximately 3.5 nm and 3–5 nm, respectively. The micellar diameter is about twice the length of the molecule and thus indicates the presence of dimeric micelles with a face-to-face stacking of the aromatic basal planes. Further apparent evidence for the formation of in-plane dimeric micelles was provided by topochemical polymerization of the sheets. Polymerization of the diacetylene groups by irradiation of the solution with UV light for 6 h yielded only dimers (see Figure S1 in the Supporting Information). This result demonstrates that the primary structure of the 2D sheets consists of dimeric micelles in which the two aromatic planes within the micellar core face one another in a slipped π–π stack for efficient dimerization of the diacetylene groups.[10]

To further confirm the primary structure of the 2D aggregates, we conducted vapor pressure osmometry (VPO) measurements in 1,4-dioxane in the concentration range of 6.1 to 17.7 $g\,kg^{-1}$ (sample/solvent). The molecular weight of the primary aggregate was measured to be 3617.3 Da, which is twice that of the single molecule (1772.2 Da; see Figure S2) and indicative of the formation of a dimeric aggregate. To gain insight into the packing arrangement of the dimeric micelles, we performed molecular-modeling experiments through quantum-mechanical calculations with the GAMESS software (Figure 2d). Energy minimization showed that the aromatic plane adopts a boat conformation in which the central benzene ring protrudes from the opposite side of the basal plane to that occupied by the dendrimer. The paired aromatic segments are "slipped" with respect to one another to reduce steric hindrance between the protruding benzene rings. The slipped stacking of the aromatic segments is reflected in a red-shifted absorption maximum in aqueous solution relative to that in chloroform (Figure 2c)[11] and efficient topochemical polymerization of the dimeric micelles as described above.

All of these observations indicate that **1** self-assembles through a face-to-face stacking arrangement of the flat aromatic segments into dimeric micelles with a flat aromatic core. These dimeric micelles in turn grow laterally through side-to-side hydrophobic interactions to form 2D sheets. However, the lateral association of the dimeric micelles leads to in-plane defects as a result of the weak lateral interactions between the very thin aromatic cores owing to the slipped packing arrangement. Thus, porous sheets are formed. This weak lateral association of the micelles is also reflected in the formation of flexible sheets.

To investigate the role of the dimeric stacking of the aromatic planes in the formation of the 2D porous sheets, we modified the molecular structure. With the aim of interfering with the dimeric stacking of the aromatic planes, we replaced the monosubstituted aromatic segment with a basal plane disubstituted at the two opposite faces to form **2** (Figure 1). In great contrast to **1**, **2** formed only irregular aggregates in solution (see Figure S3). This behavior implies that the dimeric stacking of the aromatic planes is essential for the formation of a well-defined 2D porous structure.

The formation of 2D sheets based on pairs of face-to-face-stacked aromatic molecules stimulated us to investigate

 © 2013 Wiley-VCH Verlag GmbH & Co. KGaA, Weinheim

whether the planar nanostructure would encapsulate flat aromatic guest molecules, such as coronene, through π–π stacking interactions in aqueous solution (Figure 2d). Indeed, the 2D sheets readily solubilized coronene in aqueous solution with preservation of their 2D structure. Upon the addition of coronene to an aqueous solution of **1**, the fluorescence intensity at 530 nm associated with the coronene emission increased until 0.5 equivalents of coronene had been added (see Figure S4).[12] Upon the further addition of coronene to the solution, the fluorescence intensity did not change, and precipitation was observed. Therefore, it can be concluded that the maximum coronene loading per amphiphilic molecule is 0.5 equivalents. This result implies that the flat conjugated aromatic guest is sandwiched between the two aromatic basal planes of the dimeric micelles through hydrophobic and π–π stacking interactions. Atomic force microscopy (AFM) images showed that the layer thickness increased from 2.1 to 2.5 nm upon the addition of coronene (Figure 3a,b). Thus, it appears that the coronene molecules, which have a flat conjugated surface, are effectively intercalated between the aromatic planes of the dimeric micelles.

We investigated the influence of coronene intercalation on the 2D structure by cryo-TEM analysis of a solution of **1** in the presence of coronene (0.5 equiv; Figure 3c). The resulting image shows large planar sheets with straight edges and thus indicates that the flexible sheets become stiff upon the intercalation of coronene and that the 2D structure is preserved. Notably, a TEM image of a cast film negatively stained with uranyl acetate shows large sheets with smoothly embossed surfaces without any noticeable nanopores (Figure 3d). This image shows that the lateral pores are closed upon the addition of coronene guest molecules. The magnified image shows that the diameter of the in-plane micelles decreases from 3.5 to 2.5 nm upon the addition of coronene (Figure 2b, inset and Figure 3d, inset; see also Figure S5) and thus indicates that the intercalation of the aromatic guests causes the in-plane micelles to become laterally more closely packed.

To corroborate the conformational change of the aromatic basal planes upon intercalation of the coronene guest, we performed molecular-modeling experiments. Energy minimization showed that the aromatic plane adopts an inverted boat conformation in which the central benzene ring protrudes from the face occupied by the dendrimer when coronene is encapsulated (Figure 2d). This inversion of the boat conformation provides an appropriate internal cavity to contain a coronene molecule. The nonslipped arrangement of the paired aromatic macrobicycles in the direction perpendicular to the basal plane is consistent with the decrease in the micellar diameter from 3.5 to 2.5 nm. These results indicate that the intercalation of the flat aromatic guest molecules increases the hydrophobicity of the aromatic segments of the dimeric micelles through both the nonslipped arrangement of the aromatic basal planes and the increased thickness of the aromatic cores. Consequently, the strengthened side-to-side hydrophobic interactions cause the primary micelles to be more closely laterally packed without in-plane porous defects and thus the formation of closed sheets (Figure 4). The enhanced lateral interactions upon guest intercalation are manifested by the change in the flexibility of the sheets, which become highly stiff.

Full recovery of the original porous sheets was observed by TEM upon removal of the coronene guest molecules by extraction with toluene. Thus, the in-plane nanopores undergo a reversible open/closed gating motion in response to external guests without affecting the 2D structure. This interesting behavior of the self-assembled porous sheets originates from the face-to-face stacking motif of the rigid flat aromatic segments of the amphiphilic molecules. The face-to-face stacking of flat aromatic units in pairs enables the

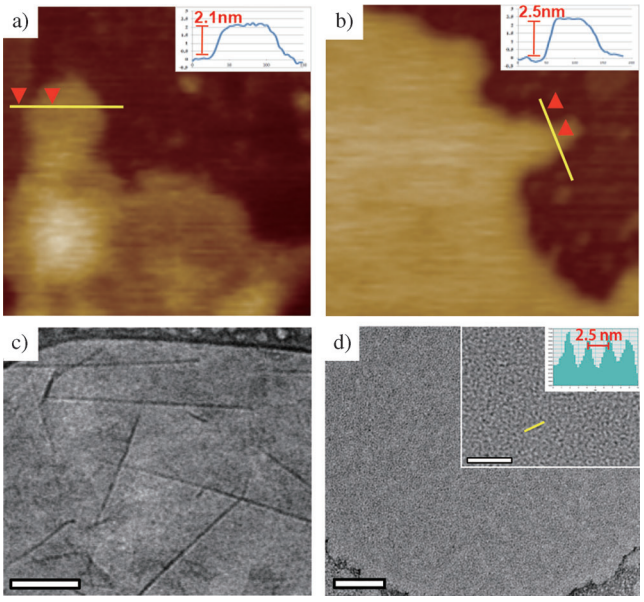

Figure 3. a,b) AFM images of **1** (a) and **1**–coronene (b; 50 μM aqueous solution, 700×700 nm²) and cross-sectional analysis of the images. c) Cryo-TEM image of a 100 μM aqueous solution of **1**–coronene (scale bar: 100 nm). d) Negatively stained TEM image of closed sheets from a 100 μM aqueous solution of **1**–coronene (scale bar: 100 nm). The inset shows a magnified image (scale bar: 20 nm) and the line profile along the yellow line.

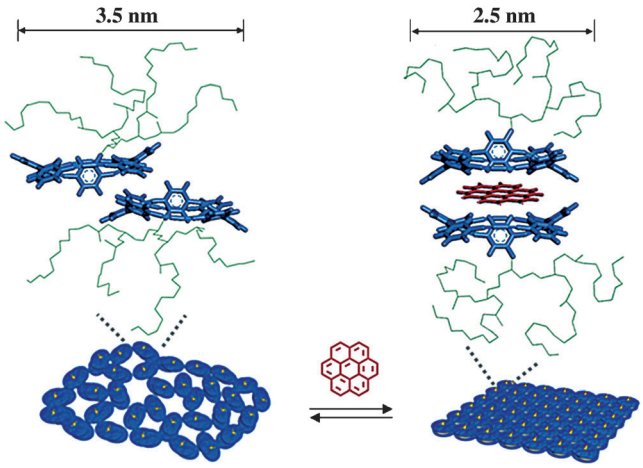

Figure 4. Schematic representation of the switch between a nanoporous sheet and a closed sheet, as triggered by the intercalation of coronene.

© 2013 Wiley-VCH Verlag GmbH & Co. KGaA, Weinheim

sandwich-type intercalation of flat aromatic guest molecules by the 2D structures. In this way, it is possible to switch between open and closed states with preservation of the 2D shape.

In conclusion, we have demonstrated that a rationally designed macrobicyclic amphiphile consisting of a hydrophilic dendron attached to the center of an aromatic plane undergoes self-assembly into a 2D structure with nanosized lateral pores through the lateral association of amphiphile dimers with a uniform diameter of 3.5 nm. The porous sheets efficiently intercalate flat aromatic molecules, such as coronene, through the conformational inversion of the basal planes of the dimeric micelles. Notably, the intercalation of a flat conjugated aromatic guest causes the reversible transformation of the porous sheets into closed sheets without sacrificing the 2D structure. This switch is also accompanied by change in the flexibility of the self-assembled 2D structure from a flexible to a rigid state. This unique supramolecular structure with switchable functionality might provide a new strategy for the design of intelligent materials with simultaneous biological and electrooptical functions. In particular, the reversible switching of the pores opens up the possibility of pumping molecules of interest out of the internal pores of such 2D systems.

Received: December 31, 2012
Revised: April 12, 2013
Published online: May 6, 2013

Keywords: host–guest systems · macrobicycles · nanoporous sheets · self-assembly · supramolecular chemistry

[1] a) Z. Huang, S.-K. Kang, M. Banno, T. Yamaguchi, D. Lee, C. Seok, E. Yashima, M. Lee, *Science* **2012**, *337*, 1521 – 1526; b) H.-J. Kim, T. Kim, M. Lee, *Acc. Chem. Res.* **2011**, *44*, 72 – 82; c) C. Wang, Z. Wang, X. Zhang, *Acc. Chem. Res.* **2012**, *45*, 608 – 618.

[2] a) T. F. A. De Greef, M. M. J. Smulders, M. Wolffs, A. P. H. J. Schenning, R. P. Sijbesma, E. W. Meijer, *Chem. Rev.* **2009**, *109*, 5687 – 5754; b) X. Yan, F. Wang, F. Huang, *Chem. Soc. Rev.* **2012**, *41*, 6042 – 6055; c) H.-J. Kim, J.-K. Kim, M. Lee, *Chem. Commun.* **2010**, *46*, 1458 – 1460; d) A. Ustinov, H. Weissman, E. Shirman, I. Pinkas, X. Zuo, B. Rybtchinski, *J. Am. Chem. Soc.* **2011**, *133*, 16201 – 16211.

[3] Z. Huang, H. Lee, E. Lee, S.-K. Kang, J.-M. Nam, M. Lee, *Nat. Commun.* **2011**, *2*, 459.

[4] a) Z. Tang, Z. Zhang, Y. Wang, S. C. Glotzer, N. A. Kotov, *Science* **2006**, *314*, 274 – 278; b) J. A. A. W. Elemans, R. R. J. Slangen, W. E. Rowan, R. J. M. Nolte, *J. Org. Chem.* **2003**, *68*, 9040 – 9049.

[5] a) E. Lee, J.-K. Kim, M. Lee, *J. Am. Chem. Soc.* **2009**, *131*, 18242 – 18243; b) S. Sim, Y. Kim, T. Kim, S. Lim, M. Lee, *J. Am. Chem. Soc.* **2012**, *134*, 20270 – 20272.

[6] J.-K. Kim, E. Lee, Y.-H. Jeong, J.-K. Lee, W.-C. Zin, M. Lee, *J. Am. Chem. Soc.* **2007**, *129*, 6082 – 6083.

[7] a) M. Kastler, W. Pisula, D. Wasserfallen, T. Pakula, K. Muellen, *J. Am. Chem. Soc.* **2005**, *127*, 4286 – 4296; b) A. R. A. Palmans, J. A. J. M. Vekemans, E. E. Havinga, E. W. Meijer, *Angew. Chem.* **1997**, *109*, 2763 – 2765; *Angew. Chem. Int. Ed. Engl.* **1997**, *36*, 2648 – 2651; c) J. J. van Gorp, J. A. J. M. Vekemans, E. W. Meijer, *J. Am. Chem. Soc.* **2002**, *124*, 14759 – 14769.

[8] a) M. Seo, M. A. Hillmyer, *Science* **2012**, *336*, 1422 – 1425; b) N. Zhou, F. S. Bates, T. P. Lodge, *Nano Lett.* **2006**, *6*, 2354 – 2357.

[9] a) W.-J. Liu, Y. Zhou, Q.-F. Zhou, Y. Ma, J. Pei, *Org. Lett.* **2008**, *10*, 2123 – 2126; b) S. Höger, V. Enkelmann, *Angew. Chem.* **1995**, *107*, 2917 – 2919; *Angew. Chem. Int. Ed. Engl.* **1995**, *34*, 2713 – 2716; c) Y. Tobe, N. Utsumi, K. Kawabata, K. Naemura, *Tetrahedron Lett.* **1996**, *37*, 9325 – 9328; d) J.-K. Kim, E. Lee, M.-C. Kim, E. Sim, M. Lee, *J. Am. Chem. Soc.* **2009**, *131*, 17768 – 17770.

[10] T.-J. Hsu, F. W. Fowler, J. W. Lauher, *J. Am. Chem. Soc.* **2012**, *134*, 142 – 145. Topochemical polymerization of the sheets hardly occurred at all within this experimental time range when coronene guest molecules were intercalated (see Figure S1).

[11] a) W. J. Harrison, D. L. Mateer, G. J. T. Tiddy, *J. Phys. Chem.* **1996**, *100*, 2310 – 2321; b) K. Adachi, K. Chayama, H. Watarai, *Langmuir* **2006**, *22*, 1630 – 1639; c) F. Würthner, *Chem. Commun.* **2004**, 1564 – 1579.

[12] J. Xiao, H. Yang, Z. Yin, J. Guo, F. Boey, H. Zhang, Q. Zhang, *J. Mater. Chem.* **2011**, *21*, 1423 – 1427.

 © 2013 Wiley-VCH Verlag GmbH & Co. KGaA, Weinheim